ACS PHYSICAL CHEMISTRY Au
AN OPEN ACCESS JOURNAL OF THE AMERICAN CHEMICAL SOCIETY

pubs.acs.org/physchemau

Article

Polarity-Driven Isomerization of a Hydroxynaphthalimide-Containing Spiropyran at Room Temperature

Yasuhiro Shiraishi,* Keiichiro Yomo, and Takayuki Hirai

Cite This: *ACS Phys. Chem Au* 2023, 3, 290–298

Read Online

ACCESS | Metrics & More | Article Recommendations | Supporting Information

ABSTRACT: Design of spiropyrans showing spontaneous isomerization driven by the polarity of solvents is an important consideration for the synthesis of optical sensory materials. Although some spiropyrans undergo polarity-driven isomerization, they must be heated owing to the high activation energy required for isomerization. In this study, we describe that a spiropyran containing a hydroxynaphthalimide unit (**1**) exhibits a polarity-driven isomerization at room temperature. It exists as a colorless spirocyclic (SP) form in less polar solvents but is isomerized to a colored merocyanine (MC) form in polar solvents. The equilibrium amount of the MC form increases with an increase in the polarity of solvents. The MC form involves two resonance structures—the quinoidal and zwitterionic forms. In polar media, the zwitterionic form dominates mainly owing to solvation by polar molecules. Solvation stabilizes the negative charge of the zwitterionic form and decreases its ground state energy, thereby enhancing SP → MC isomerization. The SP ⇌ MC isomerization terminates within barely 30 s even at room temperature because the naphthol moiety with high π-electron density lowers the activation energy for the rate-determining rotational step.

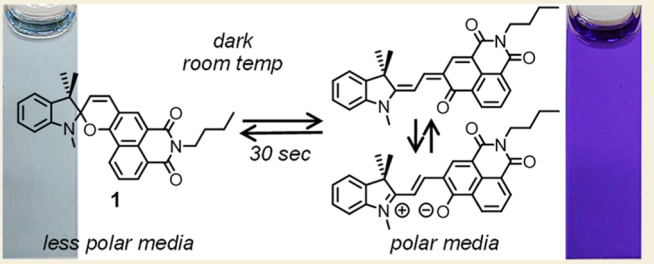

KEYWORDS: *spiropyran, isomerization, polarity, naphthalimide, merocyanine*

INTRODUCTION

Spiropyrans are a family of photochromic dyes that have been intensively studied over 50 years (Scheme 1).[1] They generally exist in solvents as colorless spirocyclic (SP) forms. They undergo isomerization to produce the colored merocyanine (MC) form by absorbing ultraviolet (UV) light and are reverted to the SP form by absorbing visible light.[2,3] The dramatic color change with the photochromism has opened up the application of spiropyrans to several kinds of optical materials such as switches,[4] memories,[5] and sensors.[6−8] The SP ⇌ MC isomerization can be initiated using other stimuli involving pH,[9] temperature,[10] cations,[11,12] anions,[13] viscosity,[14] and mechanical forces[15] even under the dark conditions. Creating spiropyrans that exhibit reversible isomerization by external stimuli is an important consideration for newer applications.

Scheme 1. Reversible SP ⇌ MC Isomerization of Spiropyrans

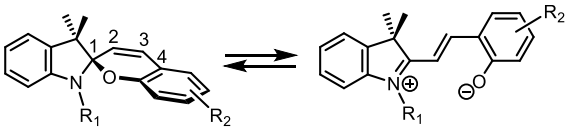

Polarity of the solvent is one of the most familiar and easy-to-handle stimuli for promoting isomerization. Previous reports revealed that some spiropyrans (Scheme 2) containing a phenol moiety with electron-withdrawing substituents such as

Scheme 2. Spiropyrans Used in This Work (1, 6, and 8)[a]

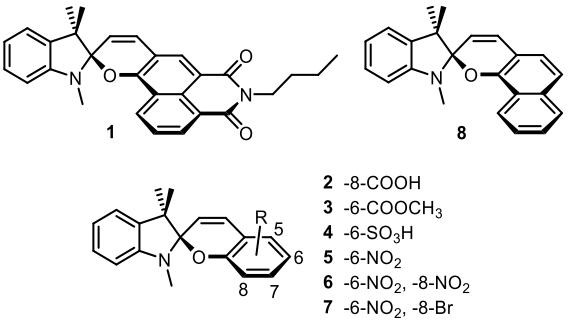

[a]Reported spiropyrans (**2**−**7**) exhibiting polarity-driven SP ⇌ MC isomerization.

Received: November 22, 2022
Revised: January 11, 2023
Accepted: January 23, 2023
Published: January 31, 2023

−COOH (**2**),[16] −$COOCH_3$ (**3**),[17] −SO_3H (**4**),[18] and −NO_2 (**5**),[19] when dissolved in polar solvents, are isomerized to the MC form under dark conditions, even though they exist in the SP form in less polar solvents. In less polar media (Scheme 3a),

Scheme 3. Ground State Potential Surface for SP ⇌ MC Isomerization of Spiropyrans

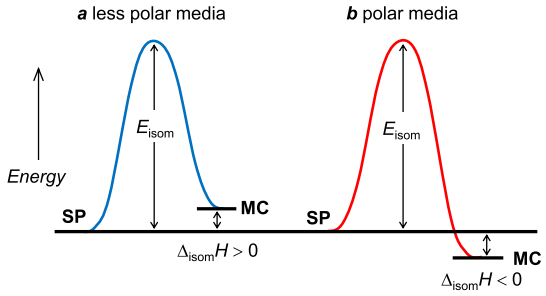

the ground state energy of the MC form of these spiropyrans is at a level higher than that of the SP form.[20] The positive enthalpy change ($\Delta_{isom}H > 0$) suppresses SP → MC isomerization. However, in polar media (Scheme 3b), the ground state energy of the MC form is decreased to below the level of the SP form ($\Delta_{isom}H < 0$) owing to stabilization of the negative charge by electron-withdrawing substituents.[21] This promotes SP → MC isomerization even under dark conditions. However, for these spiropyrans, the decrease in the ground state energy of the MC form is insufficient ($\Delta_{isom}H \sim -5$ kJ mol^{-1}), where the equilibrium amounts of the MC form are at most ∼50% even in polar media.[19] For further stabilization of the MC form in polar media, introducing multiple electron-withdrawing substituents into the phenol moiety (**6**,[22] **7**,[23] Scheme 2) is effective: they have more negative $\Delta_{isom}H$ (∼−15 kJ mol^{-1}) and achieve almost 100% of equilibrium MC amounts. Therefore, incorporating an electron-deficient phenol moiety is considered essential to synthesize the spiropyrans exhibiting polarity-driven SP → MC isomerization.

A problem involving SP ⇌ MC isomerization of spiropyrans at a ground state potential surface is that, as shown in Scheme 3, spiropyrans usually have high activation energy (E_{isom}) for isomerization (∼100 kJ mol^{-1}).[16,24,25] This results in slow isomerization; the time to achieve the SP ⇌ MC equilibrium at room temperature generally requires more than 1 h.[19,21,25] The SP → MC isomerization involves several steps such as cleavage of the spiro C_1−O bond followed by cis → trans rotation around the C_2=C_3 and C_1−C_2 bonds (Scheme 1),[13,20,26] where the rotation around the C_2=C_3 bond is considered the rate-determining step. Therefore, the design of spiropyrans with low E_{isom} is important for rapid isomerization at room temperature. A recent theoretical study based on density functional theory (DFT) calculation predicted that a fused aromatic moiety such as naphthol, when replaced with a phenol moiety of spiropyran, decreases E_{isom}.[27] A fused aromatic ring with a high electron density suppresses the electron transfer from the indoline moiety and decreases the π-bond order of the C_2=C_3 bond in the transition state. This suggests that incorporating an electron-deficient fused aromatic moiety is a possible approach to the design of spiropyrans promoting a rapid polarity-driven isomerization.

Naphthalimide is a fluorescent dye with high chemical, photochemical, and thermal stability.[28] Its application to several functional materials such as optoelectronic devices,[29] sensors,[30] and DNA-targeted binders[31] has been studied extensively. A notable feature of naphthalimide is that it contains a fused naphthalene ring and behaves as an electron acceptor owing to the electron-withdrawing imide moiety.[28] Therefore, we hypothesized that a hydroxynaphthalimide moiety, if incorporated within the structure, would produce a spiropyran with highly stabilized MC form together with low E_{isom} for isomerization.

In the present work, we designed a spiropyran containing a hydroxynaphthalimide moiety (**1**, Scheme 2). We found that it undergoes a polarity-driven rapid SP ⇌ MC isomerization even at room temperature. In less polar media, **1** is almost colorless owing to the SP form. An increase in the polarity of solvents elicits a gradual coloration owing to the formation of the MC form, where the equilibrium MC amount can be changeable from 9% in toluene to 99% in DMSO. Equilibrium analysis and DFT calculations reveal that the MC form of **1** is indeed highly stabilized in polar media, thus promoting spontaneous isomerization. In addition, the SP ⇌ MC equilibrium is achieved in less than 30 s even at room temperature. Time-dependent DFT (TD-DFT) calculations revealed that the naphthol ring with high π-electron density decreases E_{isom}, thus promoting rapid SP ⇌ MC isomerization.

RESULTS AND DISCUSSION

Synthesis and Optical Properties

1 was obtained by the condensation of 1,3,3-trimethyl-2-methyleneindoline and 3-formyl-4-hydroxy-*N*-butyl-1,8-naphthalimide[32,33] with 17% yield. FAB(+)-MS analysis of **1** (Figure S1, Supporting Information) shows $[\mathbf{1} + H]^+$ ion (m/z 453.2). ^1H, ^{13}C NMR, and ^1H−^1H COSY spectra (Figures S2−S4, Supporting Information) confirmed the purity of **1**. Spiropyrans bearing a dinitrophenol moiety (**6**)[22,34] and a naphthol moiety (**8**)[35] (Scheme 2) were also used for comparison of the isomerization properties.

UV−vis absorption spectra of **1** were recorded at 293 K in several organic solvents after stirring the solution for 30 min in the dark. As shown in Figure 1, **1** demonstrated a weak absorption in the visible region (500−640 nm) when dissolved in less polar solvents such as toluene, where the solution was almost colorless. This indicates that **1** mainly exists as an SP form in less polar media. However, **1** dissolved in polar

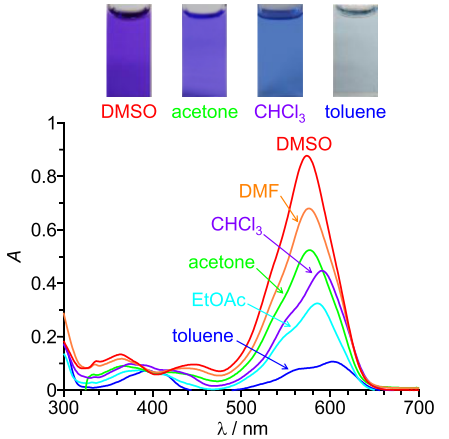

Figure 1. Absorption spectra of **1** (25 μM) measured at 293 K in different solvents after stirring for 30 min in the dark.

https://doi.org/10.1021/acsphyschemau.2c00067
ACS Phys. Chem Au 2023, 3, 290−298

solvents such as DMSO showed a purple color and increased absorbance, which might be assigned to the MC form, implying that **1** undergoes spontaneous SP → MC isomerization in polar media.

^{1}H NMR analysis of **1** was performed in deuterated solvents to confirm the formation of the MC form (Figure 2), where

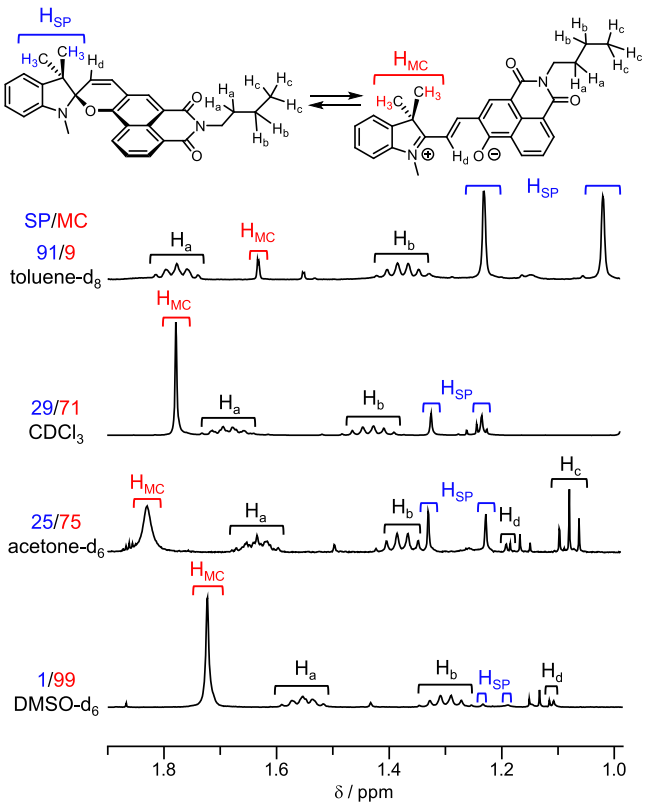

Figure 2. ^{1}H NMR spectra of **1** measured in different solvents. The equilibrium SP/MC ratio determined from their peak areas are denoted in the figure.

the full spectra are given in Figures S2 and S5−S7 (Supporting Information). Two methyl groups on the indoline moiety of the SP form are not equivalent owing to their asymmetrical structure and exhibit two separate peaks (H_{SP}).[36] In contrast, the methyl groups of the MC form show a single peak (H_{MC}) owing to their equivalent structure. The spectrum obtained in toluene-d_8 showed both H_{SP} and H_{MC} peaks, and integration of the peaks determined the SP/MC ratio to be 91:9, indicating that less polar media favorably generate the SP form. In contrast, increasing the polarity of solvents increases the H_{MC} peak while decreasing the H_{SP} peak; the SP/MC ratios were 29:71 in $CDCl_3$, 25:75 in acetone-d_6, and 1:99 in DMSO-d_6, respectively, clearly indicating that the MC form exists mainly in more polar media. Figure 3 (red) plots the MC ratio of **1** in different solvents against the normalized solvent polarity parameter, E_T^N, which is referenced to tetramethylsilane (E_T^N = 0) as nonpolar and water (E_T^N = 1) as strong polar reference solvents,[37] where the parameters used are listed in Table S1 (Supporting Information). Increasing the solvent polarity increases the MC ratio, confirming that **1** undergoes polarity-driven SP → MC isomerization.

As reported,[22] dye **6** also exhibits a polarity-driven SP → MC isomerization; no absorption is observed in the visible region in less polar media, but the MC absorbance (460−600

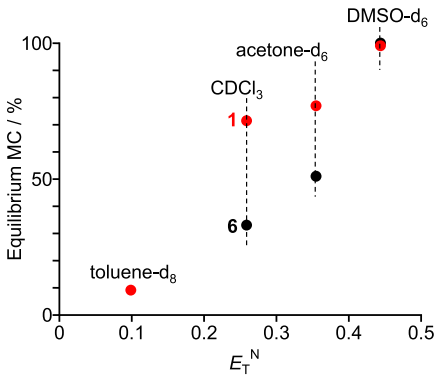

Figure 3. Plots of the equilibrium MC ratio of **1** and **6** in different solvents determined by ^{1}H NMR against the normalized solvent polarity scale (E_T^N), where the E_T^N values for toluene, $CHCl_3$, acetone, and DMSO are used.

nm) increases in more polar media (Figure S8, Supporting Information). As shown in Figure 3 (black), ^{1}H NMR analysis of **6** (Figure S9, Supporting Information) reveals that the equilibrium MC ratio shows a tendency similar to that of **1** (red), indicating that these dyes show a similar polarity dependence. In contrast, as demonstrated in Figure S10 (Supporting Information), dye **8** displays almost no absorption in the visible region even in polar media. These results indicate that the electron-deficient hydroxynaphthalimide moiety of **1** triggers spontaneous SP → MC isomerization in polar solvents.

Spiropyrans usually undergo SP ⇌ MC photoisomerization upon absorbing UV or visible light (Scheme 1).[2] However, **1** does not undergo photoisomerization. As presented in Figure S11 (Supporting Information), there is no change observed in the absorption spectra for **1** in either toluene or MeCN solvents when photoirradiated by UV or visible light.[38,39] In Figure S12 (Supporting Information), photoexcitation of toluene containing **1** (SP form exists mainly) at 375 nm results in an emission centered at 435 nm, which is ascribed to the fluorescence from the excited-state naphthalimide moiety.[33] In contrast, photoexcitation of MeCN containing **1** (where the MC form predominates) at 440 and 590 nm shows emissions centered at 512 and 625 nm, both of which might be ascribed to the fluorescence from the excited-state of the entire **1** molecule. These findings indicate that photoexcitation of both SP and MC forms of **1** leads to a loss of their excited energy via the fluorescence emission, as observed for related molecules,[40,41] resulting in no photochromic behavior.

Stabilization of MC Form

The SP → MC isomerization of **1** is triggered by stabilization of the MC form in polar media, similar to the case for the related spiropyrans.[16−19,22,23] To clarify this, equilibrium absorption experiments were performed. The relationship between the thermodynamic equilibrium constants (K_{eq}) and the equilibrium concentrations of the SP and MC forms is as follows[42]

$$K_{eq} = \frac{[MC]_{eq}}{[SP]_{eq}} \quad (1)$$

$$C_T = [SP]_{eq} + [MC]_{eq} = \frac{A_{MC}}{\varepsilon_{MC}}\left(1 + \frac{1}{K_{eq}}\right) \quad (2)$$

https://doi.org/10.1021/acsphyschemau.2c00067
ACS Phys. Chem Au 2023, 3, 290−298

Table 1. Equilibrium Data for SP → MC Isomerization of Spiropyrans (1, 6) under Dark Conditions

spiropyran	solvent	ε_{MC}/L mol^{-1}cm^{-1}[a]	temperature/K	K_{eq}[b]	$\Delta_{isom}H$/kJ mol^{-1}
1	toluene	8.67 × 10^4	293	0.116	−0.77 ± 0.54
			303	0.114	
			313	0.113	
			323	0.113	
	acetone	3.67 × 10^4	293	4.12	−16.6 ± 0.2
			303	3.34	
			313	2.27	
			323	2.18	
	DMSO	6.82 × 10^4	293	23.0	−20.4 ± 0.6
			303	17.3	
			313	13.2	
			323	10.6	
6	DMSO	2.00 × 10^4	283	20.4	−17.9 ± 0.3
			303	11.4	
			323	8.00	

[a]At 293 K. [b]Determined after stirring the solutions for 4 h (**1**) and 48 h (**6**).

C_T is the total concentration of **1**, and A_{MC} and ε_{MC} are the absorbance and molar extinction coefficient of the MC form, respectively. The ε_{MC} values in the respective solvents were determined using the Lambert−Beer equation with the path length of the cell (l)

$$A_{MC} = \varepsilon_{MC}[MC]_{eq}l \quad (3)$$

The $[MC]_{eq}$ was determined by the ^{1}H NMR analysis in the respective solvents (Figure 2). The solutions containing different concentrations of **1** (C_T) were stirred for 4 h at different temperatures under the dark conditions.[19] A linear relationship was observed when plotting C_T against A_{MC} (Figure S13, Supporting Information). K_{eq} values can be determined from the slopes and the ε_{MC} values. $\Delta_{isom}H$ values were calculated with the K_{eq} values using the van't Hoff equation (eq 4), as shown in Figure S14 (Supporting Information). The obtained K_{eq} and $\Delta_{isom}H$ are summarized in Table 1.

$$\frac{d \ln K_{eq}}{d(1/T)} = -\frac{\Delta_{isom}H}{R} \quad (4)$$

The value of K_{eq} of **1** in toluene is ∼0.1, but is higher in acetone (∼4.1) and DMSO (∼23). These values agree well with the equilibrium MC ratios determined by the NMR analysis (9, 75, and 99%, respectively, Figure 2), confirming the accuracy of the equilibrium analysis. $\Delta_{isom}H$ in toluene is −0.8 kJ mol^{-1}, but is decreased considerably in acetone (−17 kJ mol^{-1}), and DMSO (−20 kJ mol^{-1}). As shown in Figure 4 (red), the $\Delta_{isom}H$ values, when plotted against E_T^N, show a linear relationship. This clearly indicates that increase in the solvent polarity lowers the ground state energy of the MC form of **1** and enhance spontaneous SP → MC isomerization. It is noted that $\Delta_{isom}H$ in DMSO (−20 kJ mol^{-1}) is comparable to that of **6** in DMSO (−18 kJ mol^{-1}), indicating that the incorporation of a hydroxynaphthalimide moiety is effective in stabilizing the MC form.

DFT calculations were carried out to further confirm the stabilization of the MC form of **1** in polar solvents. Although several isomers of the MC form exist, the TTC form (Scheme 1 right), which has a trans−trans−cis conformation around the C_1−C_2, C_2−C_3, and C_3−C_4 bonds, has been considered the most stable MC structure.[26] We calculated the ground state energies of the SP and TTC forms of **1** within the Gaussian 16 program, where the polarizable continuum model (PCM) was used to consider the polarity effect.[43] Figure 4 (black) summarizes the calculated ground state energies of the TTC form relative to that of the SP form under different PCM conditions. The relative TTC energy decreases with an increase in polarity of the PCM parameter. This tendency agrees well with that of the $\Delta_{isom}H$ values (red). The above equilibrium analysis and the DFT calculation results clearly indicate that the lowered ground state energy of the MC form of **1** in more polar media triggers SP → MC isomerization.

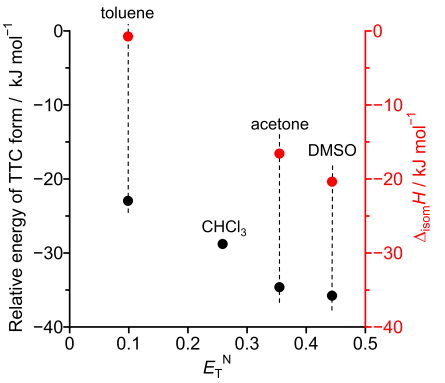

Figure 4. Plots of E_T^N parameter vs $\Delta_{isom}H$ of **1** obtained in different solvents by the equilibrium absorption analysis and the relative energy of the TTC form of **1** to the SP form calculated under different PCM conditions.

Resonance Structures of MC Form

The reason for the stabilization of the MC form of **1** in more polar solvents (Figure 4) must be clarified. According to Figure 1, the MC absorption band of **1** shows a hypsochromic shift in more polar solvents, as observed for the related spiropyrans.[21,44] Figure 5 plots the maximum wavelengths (λ_{max}) of the MC absorption of **1** in different solvents against the E_T^N parameter, where the absorption spectra of **1** in all of the solvents used are provided in Figure S15 (Supporting Information). A linear correlation indicates that the MC form of **1** has two resonance structures (Figure 6a):[44−47] the quinoidal form is dominant mainly in less polar media, while the contribution of zwitterionic form becomes larger in more

https://doi.org/10.1021/acsphyschemau.2c00067
ACS Phys. Chem Au 2023, 3, 290−298

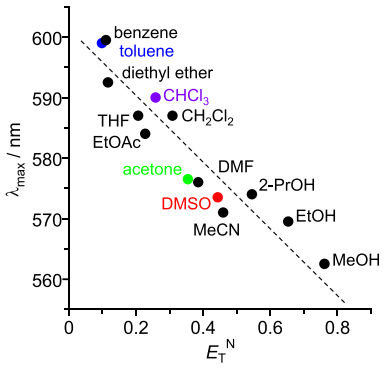

Figure 5. Relationship between the maximum wavelengths of the MC absorption band of **1** in different solvents and E_T^N parameter.

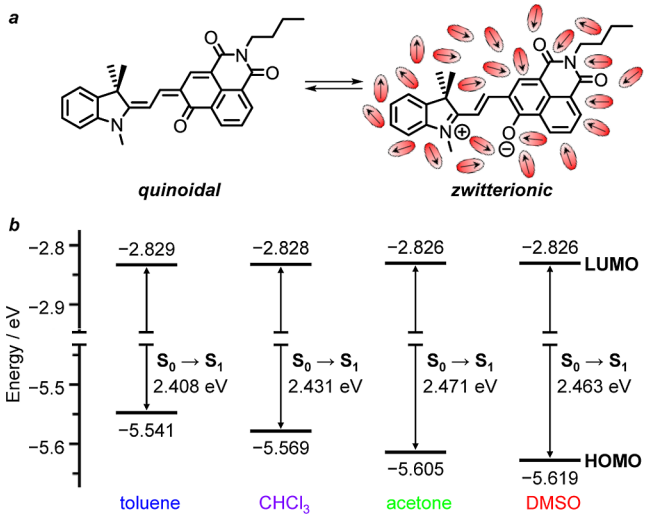

Figure 6. (a) Resonance structures of the TTC form of **1**. (b) HOMO and LUMO levels of the TTC form of **1** calculated under different PCM conditions (TD-DFT/B3LYP/6-31+G).

polar media. This is because the zwitterionic form has a lower HOMO level: therefore, increased contribution of the zwitterionic form increases the HOMO−LUMO gap and results in the hypsochromic shift of the MC absorption band.

Time-dependent DFT (TD-DFT) calculations of the TTC form of **1** were performed to clarify their electronic structures under different PCM conditions. As summarized in Table S2 (Supporting Information), the electronic excitation of the TTC form mainly consists of a HOMO → LUMO transition ($S_0 \rightarrow S_1$) under all PCM conditions. As shown in Figure 6b, the LUMO levels of the TTC forms are similar under all PCM conditions, but the HOMO levels decrease with an increase in polarity of PCM. Therefore, the HOMO−LUMO gap increases with the increase in the polarity. This agrees well with the hypsochromic shift of **1** (Figure 5), indicating that the contribution of the zwitterionic form indeed becomes larger in more polar media.[44−47] Notably, the hypsochromic shift (Figure 5) is consistent with the decrease in ground state energy of the TTC form (Figure 4), suggesting that the zwitterionic form has a ground state energy lower than the quinoidal form. In more polar media, solvation of the MC form by polarized solvent molecules creates the polarized zwitterionic form (Figure 6a, right).[45,46] This may stabilize the negative charge of the form and lower the ground state energy,[44] thus enhancing the SP → MC isomerization. The above findings indicate that the polarity-driven formation of the zwitterionic form lowers the ground state energy of the MC form and triggers SP → MC isomerization.

Rapid Isomerization

Another notable feature of **1** is the rapid isomerization even at room temperature. Figure 7a,b shows changes in absorption

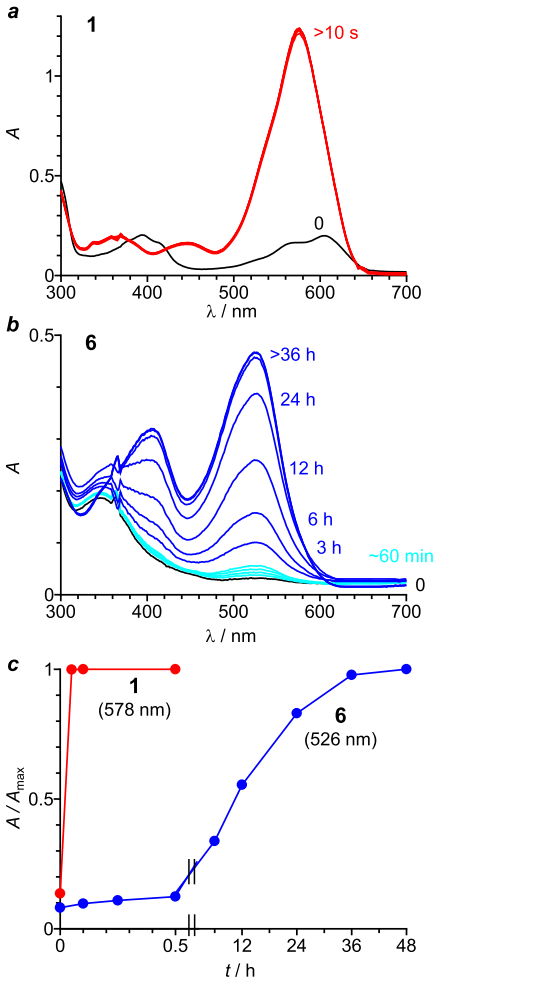

Figure 7. Change in absorption spectra of (a) **1** (25 μM) and (b) **6** (25 μM) in DMSO at 293 K with time. The dye (500 μM) was dissolved in toluene (0.1 mL), and the measurement were started immediately after the addition of DMSO (1.9 mL). The spectra at 0 h are those of toluene solutions (25 μM). (c) Change in the relative absorbance of **1** at 578 nm and **6** at 526 nm, respectively.

spectra of **1** and **6**, respectively, measured at 293 K under dark conditions. Each of the respective dyes was dissolved in toluene (0.1 mL), and spectral measurement was started after the addition of DMSO (1.9 mL) to the solutions. In the case of **6** (Figure 7c), the MC absorbance increases very slowly and reaches equilibrium after ∼36 h owing to its high E_{isom}. Therefore, heating the solution is necessary for rapid SP → MC isomerization.[22] In contrast, in the case of **1** (Figure 7c), the MC absorbance increases very rapidly and reaches equilibrium within 10 s, indicating that **1** facilitates rapid SP → MC isomerization even at room temperature. Figure S16 (Supporting Information) presents the change in absorption spectra of **1** in DMSO (0.1 mL) after the addition of toluene (1.9 mL). The MC absorbance decreases immediately by the addition of toluene and reaches equilibrium within 30 s. This

https://doi.org/10.1021/acsphyschemau.2c00067
ACS Phys. Chem Au 2023, 3, 290−298

Scheme 4. Proposed Pathway for Isomerization

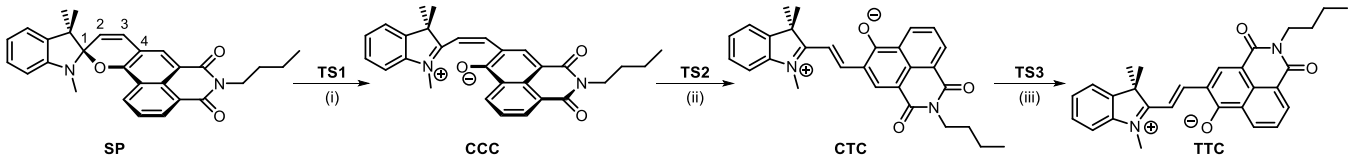

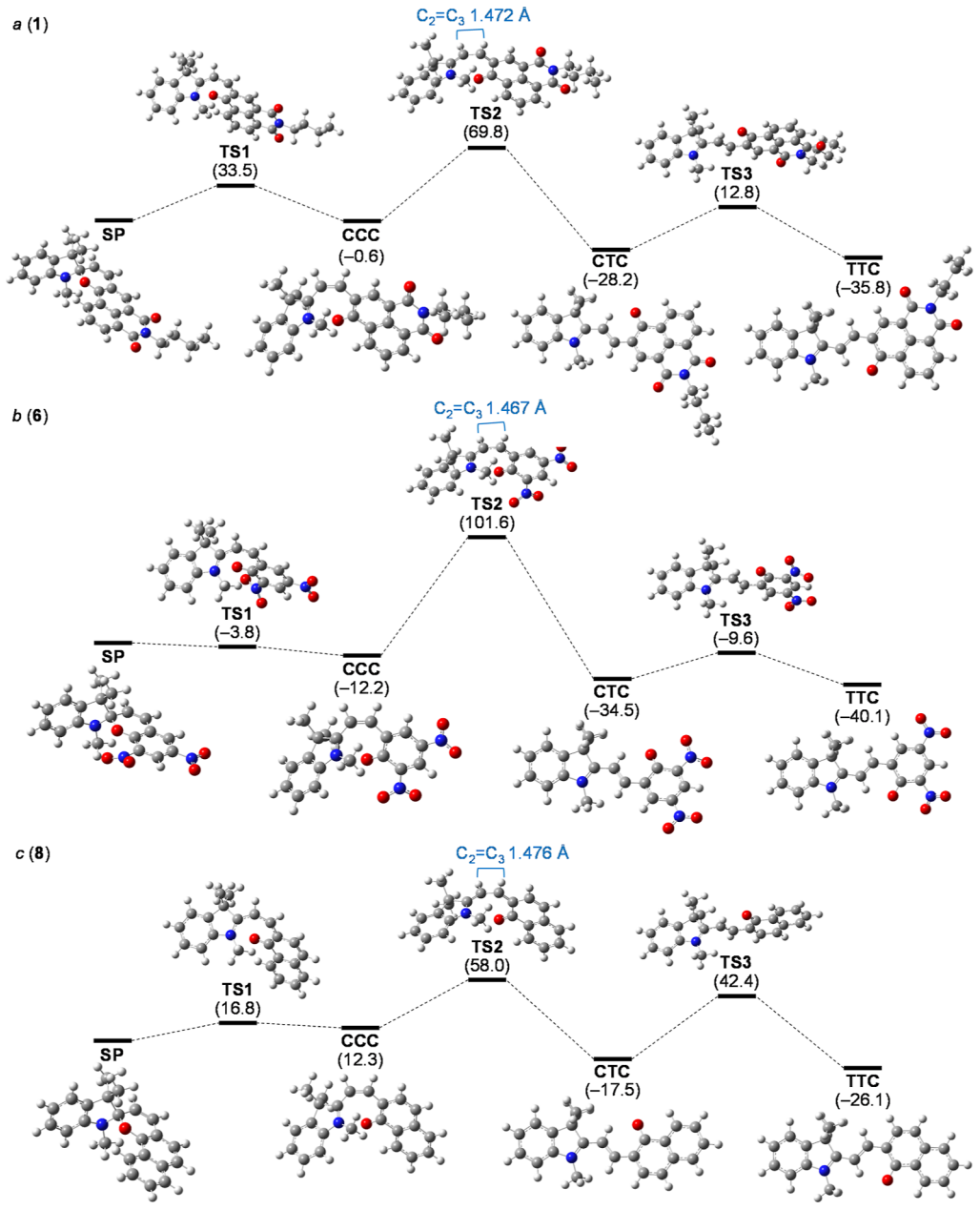

Figure 8. Ground state potential surface for isomerization of (a) **1**, (b) **6**, and (c) **8**, calculated using DMSO as PCM (TD-DFT/B3LYP/6-31+G). The numbers in parentheses are the energies (kJ mol^{-1}) relative to those of the SP forms. The blue texts are the C_2═C_3 bond lengths.

indicates that MC → SP isomerization of **1** also occurs very rapidly, confirming a low E_{isom} for isomerization of **1**.

Activation Energy for Isomerization

The E_{isom} values of spiropyrans can be generally determined by kinetic measurements (see text in the Supporting Information).[19] As shown in Figure S17 (Supporting Information), the kinetic absorption measurements of **6** for SP → MC isomerization in MeCN at different temperatures (313−333 K), and the corresponding Arrhenius plots of the obtained kinetic constants determined E_{isom} of **6** to be 102.5 kJ mol^{-1}. However, in the case of **1**, SP → MC isomerization at around room temperature occurs very rapidly (Figure 7c). Therefore, as shown in Figure S18 (Supporting Information), the kinetic measurements were performed at lower temperatures (268−278 K). This determined E_{isom} of **1** to be 50.6 kJ mol^{-1}, which is much lower than that of **6**, confirming low E_{isom} of **1**.

https://doi.org/10.1021/acsphyschemau.2c00067
ACS Phys. Chem Au 2023, 3, 290−298

DFT calculations were performed to further confirm the low E_{isom} of **1**. The SP → MC isomerization usually occurs through three steps[13,20,26] via the CCC and CTC intermediates, as summarized in Scheme 4: (i) the cleavage of the C_1−O bond for the SP form gives the CCC form through a TS1 transition state; (ii) cis → trans isomerization around the C_2=C_3 bond gives the CTC form through a TS2 state; and (iii) cis → trans isomerization around the C_1−C_2 bond generates the TTC form through a TS3 state. Step (ii) is the rate-determining reaction for isomerization.[13,20,26] The respective ground states were optimized by the DFT calculations with DMSO as PCM, and the transition states were optimized using the TS Berny method.[48] Figure 8 presents the optimized structures of the ground and transition states of **1**, **6**, and **8** and their relative energies with respect to the SP form. The results clearly indicate that, as reported,[13,20,26] TS2 (ii) indeed requires the highest energy for isomerization. The TS2 energy of **6** (101.6 kJ mol^{-1}) is similar to the experimental value (102.5 kJ mol^{-1}) determined by kinetic absorption measurements (Figure S17, Supporting Information), confirming the accuracy of the calculated E_{isom} value. The TS2 energy of **1** (69.8 kJ mol^{-1}) is also similar to the experimental value (50.6 kJ mol^{-1}), and is much lower than that of **6**. This clearly indicates that the lower TS2 energy of **1** facilitates rapid isomerization. The TS2 consists of the rotation around the C_2=C_3 bond (Scheme 4);[13] therefore, the C_2=C_3 bond strength is crucial for its energy.[49] As denoted in Figure 8, the calculated C_2=C_3 length of the TS2 state of **1** is 1.472 Å, while the length of **6** is 1.467 Å. This indicates that **1** indeed has a longer (weaker) C_2=C_3 bond and, hence, results in lower E_{isom}.

As predicted,[27] incorporating a fused aromatic unit decreases E_{isom} of spiropyrans: the high-π-electron-density unit suppresses the electron transfer from the indoline moiety and decreases the π-bond order of the C_2=C_3 bond in the TS2 state. Figure 8c shows the calculation results of **8** incorporating a naphthol moiety (Scheme 2). The results indicate that **8** also has a long C_2=C_3 bond (1.476 Å) and a low TS2 energy (58.0 kJ mol^{-1}), similar to those of **1**, confirming that introducing a fused naphthol ring decreases the TS2 energy. Table S3 (Supporting Information) summarizes the dipole moment for the ground and transition states of **1**, **6**, and **8**. TS2 of **6** has a high dipole moment (9.524 Debye), implying that electron transfer from the indoline moiety to the dinitrophenol moiety creates a charge-transferred electronic structure. In contrast, TS2 of **1** and **8** have lower dipole moments (2.927 and 4.515 Debye, respectively), indicating that the electron transfer from the indoline moiety is suppressed by introducing a naphthol moiety with high electron density. Therefore, this weakens the C_2=C_3 bond and lowers the rotational TS2 energy, resulting in rapid isomerization of **1**.

The activation entropies ($\Delta S^{\ddagger}$) for SP → MC isomerization of **1** and **6**, calculated from the frequency factors obtained by the Arrhenius plots[50] (Figures S17 and S18, Supporting Information), were −65.0 J K^{-1} mol^{-1} (298 K) and 24.9 J K^{-1} mol^{-1} (298 K), respectively (see text in the Supporting Information). The $\Delta S^{\ddagger}$ values depend on the ground state conformation.[14,51] The C_1−O cleaved CCC intermediate of **6** may have a charge-transferred rigid structure with a low entropy, whereas the CCC intermediate of **1** may have a flexible structure with a high intrinsic entropy, as suggested by the dipole moment of the CCC intermediate of **1** lower than that of **6** (Table S3, Supporting Information). The rotation around the C_2=C_3 bond of **1** therefore decrease $\Delta S^{\ddagger}$, while that of **6** increases $\Delta S^{\ddagger}$. The results are also consistent with the C_2=C_3 length of the TS2 state of **1** longer than that of **6** (Figure 8a,b).

As shown in Figure S10 (Supporting Information), **8** scarcely undergo SP → MC isomerization even in polar media, because it does not contain an electron-deficient moiety and its TTC form is not stabilized sufficiently, as confirmed by the shallow ground state energy (Figure 8, right). Introducing a hydroxynaphthalimide, which is an electron-deficient fused aromatic moiety, lowers E_{isom} for isomerization, while stabilizing the TTC form. This facilitates polarity-driven rapid isomerization even at room temperature.

CONCLUSIONS

We demonstrated that a hydroxynaphthalimide-containing spiropyran (**1**) exhibits polarity-driven rapid SP ⇌ MC isomerization at room temperature. The SP → MC isomerization is driven by the ground state energy of the MC form of **1** lowered in more polar media. The quinoidal MC form exists mainly in less polar media, while the zwitterionic MC form exists dominantly with the increase in solvent polarity. The stabilized negative charge of the zwitterionic MC form lowers the ground state energy and, as a result, promotes enhanced SP → MC isomerization. **1** exhibits rapid SP ⇌ MC isomerization when changing the polarity of solvents; it reaches equilibrium within 30 s even at room temperature. Introducing a hydroxynaphthalene moiety with high π-electron density suppresses intramolecular charge transfer in the transition state. This decreases π-bond order of the C_2=C_3 bond and lowers the activation energy for rotational motion. The molecular design based on the introduction of an electron-deficient, fused aromatic moiety may contribute to the development of functional spiropyrans.

EXPERIMENTAL SECTION

General

All reagents were purchased from Wako and Aldrich and used without further purification. The dyes **6** and **8** were obtained according to the procedure reported previously.[22,35] 3-Formyl-4-hydroxy-*N*-butyl-1,8-naphthalimide was synthesized according to the literature procedure.[40,41] The spectral measurements were carried out under aerated conditions for the sake of data reproducibility.

Synthesis of Dye 1 [5-Butyl-1′,3′,3′-trimethyl-4*H*-spiro[benzo[de]pyrano-[2,3-g]isoquinoline-10,2′-indoline]-4,6(5*H*)-dione]

1,3,3-Trimethyl-2-methyleneindoline (329 mg, 1.9 mmol) and 3-formyl-4-hydroxy-*N*-butyl-1,8-naphthalimide (538 mg, 1.8 mmol) were stirred in EtOH (20 mL) at 343 K for 16 h. The resulting solution was concentrated by evaporation, and the residue was purified by a silica gel column chromatography using *n*-hexane/ethyl acetate (1:1 v/v) as an eluent, affording **1** as a dark green solid (161 mg, 17%). ^{1}H NMR (400 MHz, DMSO-d_6, TMS) δ (ppm): 8.62 (1H, s), 8.46 (1H, d, J = 7.6 Hz), 8.30 (1H, d, J = 7.6 Hz), 7.67 (1H, d, J = 8.0 Hz), 7.56 (1H, d, J = 8.0 Hz), 7.52 (1H, m), 7.45 (1H, m), 7.34 (1H, m), 3.99 (3H, m), 3.78 (3H, s), 1.72 (6H, s), 1.51−1.60 (2H, m), 1.25−1.35 (2H, m), 1.10−1.16 (1H, m), 0.86−0.91 (3H, m). ^{13}C NMR (400 MHz, DMSO-d_6, TMS) δ (ppm): 167.5, 164.3, 163.3, 142.9, 142.6, 132.2, 132.1, 132.0, 130.8, 130.2,129.2, 129.0, 126.8, 125.2, 123.0, 122.3, 122.2, 120.5, 119.7, 113.0, 50.5, 32.6, 30.4, 30.3, 27.6, 20.3, 14.4, 14.3. FAB(+)-MS m/z: calcd for $C_{29}H_{29}N_2O_3^+$ [**1** + H]$^+$, 453.2173; found, 453.2174.

https://doi.org/10.1021/acsphyschemau.2c00067
ACS Phys. Chem Au 2023, 3, 290−298

■ ASSOCIATED CONTENT

Supporting Information

The Supporting Information is available free of charge at https://pubs.acs.org/doi/10.1021/acsphyschemau.2c00067.

Instruments; DFT calculations; kinetic absorption measurements (text); characterization data of **1**; ^{1}H NMR of **1**; absorption spectra of **6**; ^{1}H NMR of **6**; absorption spectra of **8**; absorption spectra of **1** upon photoirradiation; fluorescence spectra of **1**; equilibrium absorption data; absorption spectra of **1** in different solvents; time-dependent change in absorption spectra in toluene; kinetic absorption data; Cartesian coordinates for **1**, **6**, and **8**; E_T^N used; TD-DFT calculation results; calculated dipole moments; and references (PDF)

■ AUTHOR INFORMATION

Corresponding Author

Yasuhiro Shiraishi − *Research Center for Solar Energy Chemistry and Division of Chemical Engineering, Graduate School of Engineering Science, Osaka University, Toyonaka 560-8531, Japan*; orcid.org/0000-0003-1812-0644; Email: shiraishi.yasuhiro.es@osaka-u.ac.jp

Authors

Keiichiro Yomo − *Research Center for Solar Energy Chemistry and Division of Chemical Engineering, Graduate School of Engineering Science, Osaka University, Toyonaka 560-8531, Japan*

Takayuki Hirai − *Research Center for Solar Energy Chemistry and Division of Chemical Engineering, Graduate School of Engineering Science, Osaka University, Toyonaka 560-8531, Japan*

Complete contact information is available at: https://pubs.acs.org/10.1021/acsphyschemau.2c00067

Author Contributions

All the authors contributed equally. CRediT: **Keiichiro Yomo** data curation (equal), formal analysis (equal), investigation (equal), writing-original draft (equal).

Notes

The authors declare no competing financial interest.

■ ACKNOWLEDGMENTS

This work was supported by a Grant-in-Aid for Exploratory Research (no. 20K21109) from the Ministry of Education, Culture, Sports, Science and Technology, Japan (MEXT).

■ REFERENCES

(1) Hirshberg, Y.; Fischer, E. Photochromism and Reversible Multiple Internal Transitions in Some Spiropyrans at Low Temperatures. Part I. *J. Chem. Soc.* **1954**, 297−303.

(2) Berkovic, G.; Krongauz, V.; Weiss, V. Spiropyrans and Spirooxazines for Memories and Switches. *Chem. Rev.* **2000**, *100*, 1741−1754.

(3) Kortekaas, L.; Browne, W. R. The Evolution of Spiropyran: Fundamentals and Progress of an Extraordinarily Versatile Photochrome. *Chem. Soc. Rev.* **2019**, *48*, 3406−3424.

(4) Vlassiouk, I.; Park, C.-D.; Vail, S. A.; Gust, D.; Smirnov, S. Control of Nanopore Wetting by a Photochromic Spiropyran: A Light-Controlled Valve and Electrical Switch. *Nano Lett.* **2006**, *6*, 1013−1017.

(5) Frolova, L. A.; Rezvanova, A. A.; Lukyanov, B. S.; Sanina, N. A.; Troshin, P. A.; Aldoshin, S. M. Design of Rewritable and Read-Only Non-Volatile Optical Memory Elements Using Photochromic Spiropyran-Based Salts as Light-Sensitive Materials. *J. Mater. Chem. C* **2015**, *3*, 11675−11680.

(6) Zhu, L.; Wu, W.; Zhu, M.-Q.; Han, J. J.; Hurst, J. K.; Li, A. D. Q. Reversibly Photoswitchable Dual-Color Fluorescent Nanoparticles as New Tools for Live-Cell Imaging. *J. Am. Chem. Soc.* **2007**, *129*, 3524−3526.

(7) Shiraishi, Y.; Adachi, K.; Itoh, M.; Hirai, T. Spiropyran as a Selective, Sensitive, and Reproducible Cyanide Anion Receptor. *Org. Lett.* **2009**, *11*, 3482−3485.

(8) Shiraishi, Y.; Sumiya, S.; Hirai, T. Highly Sensitive Cyanide Anion Detection with a Coumarin−Spiropyran Conjugate as a Fluorescent Receptor. *Chem. Commun.* **2011**, *47*, 4953−4955.

(9) Fissi, A.; Pieroni, O.; Angelini, N.; Lenci, F. Photoresponsive Polypeptides. Photochromic and Conformational Behavior of Spiropyran-Containing Poly(L-Glutamate)s under Acid Conditions. *Macromolecules* **1999**, *32*, 7116−7121.

(10) Minkin, V. I. Photo-, Thermo-, Solvato-, and Electrochromic Spiroheterocyclic Compounds. *Chem. Rev.* **2004**, *104*, 2751−2776.

(11) Wojtyk, J. T. C.; Buncel, P. M.; Kazmaier, E. Effects of Metal Ion Complexation on the Spiropyran-Merocyanine Interconversion: Development of a Thermally Stable Photo-Switch. *Chem. Commun.* **1998**, 1703−1704.

(12) Paramonov, S. V.; Lokshin, V.; Fedorova, O. A. Spiropyran, Chromene or Spirooxazine Ligands: Insights into Mutual Relations between Complexing and Photochromic Properties. *J. Photochem. Photobiol., C* **2011**, *12*, 209−236.

(13) Shiraishi, Y.; Yamamoto, K.; Sumiya, S.; Hirai, T. Spiropyran as a Reusable Chemosensor for Selective Colorimetric Detection of Aromatic Thiols. *Phys. Chem. Chem. Phys.* **2014**, *16*, 12137−12142.

(14) Shiraishi, Y.; Inoue, T.; Sumiya, S.; Hirai, T. Entropy-Driven Thermal Isomerization of Spiropyran in Viscous Media. *J. Phys. Chem. A* **2011**, *115*, 9083−9090.

(15) Potisek, S. L.; Davis, D. A.; Sottos, N. R.; White, S. R.; Moore, J. S. Mechanophore-Linked Addition Polymers. *J. Am. Chem. Soc.* **2007**, *129*, 13808−13809.

(16) Shimizu, I.; Kokado, H.; Inoue, E. Photoreversible Photographic Systems. VI. Reverse Photochromism of 1,3,3-Trimethyl-[Indoline-2,2′-Benzopyran]-8′-Carboxylic Acid. *Bull. Chem. Soc. Jpn.* **1969**, *42*, 1730−1734.

(17) Keum, S. R.; Roh, S. J.; Kim, S. E.; Lee, S. H.; Cho, C. H.; Kim, S. H.; Koh, K. N. Unusual Reverse Photochromic Behavior of Indolinobenzospiropyran 6-Carboxylates in Aqueous Binary Solvents. *Bull. Korean Chem. Soc.* **2006**, *27*, 187−188.

(18) Sunamoto, J.; Iwamoto, K.; Akutagawa, M.; Nagase, M.; Kondo, H. Rate Control by Restricting Mobility of Substrate in Specific Reaction Field. Negative Photochromism of Water-Soluble Spiropyran in AOT Reversed Micelles. *J. Am. Chem. Soc.* **1982**, *104*, 4904−4907.

(19) Shiraishi, Y.; Itoh, M.; Hirai, T. Thermal Isomerization of Spiropyran to Merocyanine in Aqueous Media and Its Application to Colorimetric Temperature Indication. *Phys. Chem. Chem. Phys.* **2010**, *12*, 13737−13745.

(20) Sheng, Y.; Leszczynski, J.; Garcia, A. A.; Rosario, R.; Gust, D.; Springer, J. Comprehensive Theoretical Study of the Conversion Reactions of Spiropyrans: Substituent and Solvent Effects. *J. Phys. Chem. B* **2004**, *108*, 16233−16243.

(21) Song, X.; Zhou, J.; Li, Y.; Tang, Y. Correlations between solvatochromism, Lewis acid-base equilibrium and photochromism of an indoline spiropyran. *J. Photochem. Photobiol., A* **1995**, *92*, 99−103.

(22) Hobley, J.; Malatesta, V.; Giroldini, W.; Stringo, W. π-Cloud and Non-Bonding or H-Bond Connectivities in Photochromic Spiropyrans and Their Merocyanines Sensed by ^{13}C Deuterium Isotope Shifts. *Phys. Chem. Chem. Phys.* **2000**, *2*, 53−56.

(23) Hobley, J.; Malatesta, V. Energy Barrier to TTC-TTT Isomerisation for the Merocyanine of a Photochromic Spiropyran. *Phys. Chem. Chem. Phys.* **2000**, *2*, 57−59.
(24) Suzuki, T.; Lin, F. T.; Priyadashy, S.; Weber, S. G. Stabilization of the Merocyanine Form of Photochromic Compounds in Fluoro Alcohols Is Due to a Hydrogen Bond. *Chem. Commun.* **1998**, 2685−2686.
(25) Bénard, S.; Yu, P. New Spiropyrans Showing Crystalline-State Photochromism. *Adv. Mater.* **2000**, *12*, 48−50.
(26) Cottone, G.; Noto, R.; La Manna, G. Theoretical Study of Spiropyran-Merocyanine Thermal Isomerization. *Chem. Phys. Lett.* **2004**, *388*, 218−222.
(27) Dorogan, I. V.; Minkin, V. I. Theoretical modeling of electrocyclic 2H-pyran and 2H-1,4-oxazine ring opening reactions in photo- and thermochromic spiropyrans and spirooxazines. *Chem. Heterocycl. Compd.* **2016**, *52*, 730−735.
(28) Dong, H. Q.; Wei, T. B.; Ma, X. Q.; Yang, Q. Y.; Zhang, Y. F.; Sun, Y. J.; Shi, B. B.; Yao, H.; Zhang, Y. M.; Lin, Q. 1,8-Naphthalimide-based fluorescent chemosensors: recent advances and perspectives. *J. Mater. Chem. C* **2020**, *8*, 13501−13529.
(29) Ott, I.; Xu, Y.; Liu, J.; Kokoschka, M.; Harlos, M.; Sheldrick, W. S.; Qian, X. Sulfur-substituted naphthalimides as photoactivatable anticancer agents: DNA interaction, fluorescence imaging, and phototoxic effects in cultured tumor cells. *Bioorg. Med. Chem.* **2008**, *16*, 7107−7116.
(30) Yang, Q.; Yang, P.; Qian, L.; Tong, L. Naphthalimide intercalators with chiral amino side chains: Effects of chirality on DNA binding, photodamage and antitumor cytotoxicity. *Bioorg. Med. Chem.* **2008**, *18*, 6210−6213.
(31) Banerjee, S.; Kitchen, J. A.; Bright, S. A.; O'Brien, J. E.; Williams, D. C.; Kelly, J. M.; Gunnlaugsson, T. Synthesis, spectroscopic and biological studies of a fluorescent Pt(ii) (terpy) based 1,8-naphthalimide conjugate as a DNA targeting agent. *Chem. Commun.* **2013**, *49*, 8522−8524.
(32) Song, L.; Yang, Y.; Zhang, Q.; Tian, H.; Zhu, W. Synthesis and photochromism of naphthopyrans bearing naphthalimide chromophore: Predominant thermal reversibility in color-fading and fluorescence switch. *J. Phys. Chem. B* **2011**, *115*, 14648−14658.
(33) Guo, B.; Nie, H.; Yang, W.; Tian, Y.; Jing, J.; Zhang, X. A highly sensitive and rapidly responding fluorescent probe with a large Stokes shift for imaging intracellular hypochlorite. *Sens. Actuators, B* **2016**, *236*, 459−465.
(34) Shiraishi, Y.; Itoh, M.; Hirai, T. Rapid colorimetric sensing of cyanide anion in aqueous media with a spiropyran derivative containing a dinitrophenolate moiety. *Tetrahedron Lett.* **2011**, *52*, 1515−1519.
(35) Shiraishi, Y.; Takagi, S.; Yomo, K.; Hirai, T. Spontaneous Isomerization of a Hydroxynaphthalene-Containing Spiropyran in Polar Solvents Enhanced by Hydrogen Bonding Interactions. *ACS Omega* **2021**, *6*, 35619−35628.
(36) Natali, M.; Soldi, L.; Giordani, S. A photoswitchable Zn(II) selective spiropyran-based sensor. *Tetrahedron* **2010**, *66*, 7612−7617.
(37) Reichardt, C. Solvatochromic Dyes as Solvent Polarity Indicators. *Chem. Rev.* **1994**, *94*, 2319−2358.
(38) Shiraishi, Y.; Tanaka, K.; Shirakawa, E.; Sugano, Y.; Ichikawa, S.; Tanaka, S.; Hirai, T. Light-Triggered Self-Assembly of Gold Nanoparticles Based on Photoisomerization of Spirothiopyran. *Angew. Chem., Int. Ed.* **2013**, *52*, 8304−8308.
(39) Shiraishi, Y.; Hashimoto, M.; Chishiro, K.; Moriyama, K.; Tanaka, S.; Hirai, T. Photocatalytic dinitrogen fixation with water on bismuth oxychloride in chloride solutions for solar-to-chemical energy conversion. *J. Am. Chem. Soc.* **2020**, *142*, 7574−7583.
(40) Shiraishi, Y.; Hayashi, N.; Nakahata, M.; Sakai, S.; Hirai, T. Naphthalimide−coumarin conjugate: ratiometric fluorescent receptor for self-calibrating quantification of cyanide anions in cells. *RSC Adv.* **2017**, *7*, 32304−32309.
(41) Shiraishi, Y.; Nakatani, R.; Takagi, S.; Yamada, C.; Hirai, T. A Naphthalimide−Sulfonylhydrazine Conjugate as a Fluorescent Chemodosimeter for Hypochlorite. *Chemosensors* **2020**, *8*, 123−134.
(42) Flannery, J. B., Jr. The Photo- and Thermochromic Transients from Substituted 1′,3′,3′-Trimethylindolinobenzospiropyrans. *J. Am. Chem. Soc.* **1968**, *90*, 5660−5671.
(43) Cossi, M.; Barone, V.; Cammi, R.; Tomasi, J. Ab Initio Study of Solvated Molecules: A New Implementation of the Polarizable Continuum Model. *Chem. Phys. Lett.* **1996**, *255*, 327−335.
(44) Kalninsh, K. K. Structure and thermochromism of spiropyrans. Triplet mechanism of the thermal cleavage/closure of the pyran ring. *J. Mol. Struct.* **1998**, *39*, 642−650.
(45) Burke, K.; Riccardi, C.; Buthelezi, T. Thermosolvatochromism of Nitrospiropyran and Merocyanine Free and Bound to Cyclodextrin. *J. Phys. Chem. B* **2012**, *116*, 2483−2491.
(46) Wojtyk, J. T. C.; Wasey, A.; Kazmaier, P. M.; Hoz, S.; Buncel, E. Thermal Reversion Mechanism of N-Functionalized Merocyanines to Spiropyrans: A Solvatochromic, Solvatokinetic, and Semiempirical Study. *J. Phys. Chem. A* **2000**, *104*, 9046−9055.
(47) Botrel, A.; le Beuze, A. L.; Jacques, P.; Strub, H. Solvatochromism of a Typical Merocyanine Dye A Theoretical Investigation through the CNDO/SCI Method Including Solvatation. *J. Chem. Soc. Faraday. Trans.* **1984**, *80*, 1235−1252.
(48) Gonzalez, C.; Schlegel, H. B. Reaction Path Following in Mass-Weighted Internal Coordinates. *J. Phys. Chem.* **1990**, *94*, 5523−5527.
(49) Wazzan, N. A.; Richardson, P. R.; Jones, A. C. Cis-Trans isomerisation of azobenzenes studied by laser-coupled NMR spectroscopy and DFT calculations. *Photochem. Photobiol. Sci.* **2010**, *9*, 968−974.
(50) Zhang, S.; Zhang, Q.; Ye, B.; Li, X.; Zhang, X.; Deng, Y. Photochromism of Spiropyran in Ionic Liquids: Enhanced Fluorescence and Delayed Thermal Reversion. *J. Phys. Chem. B* **2009**, *113*, 6012−6019.
(51) Zanoni, M.; Coleman, S.; Fraser, K. J.; Byrne, R.; Wagner, K.; Gambhir, S.; Officer, D. L.; Wallace, G. G.; Diamond, D. Physicochemical Study of Spiropyran-Terthiophene Derivatives: Photochemistry and Thermodynamics. *Phys. Chem. Chem. Phys.* **2012**, *14*, 9112−9120.

https://doi.org/10.1021/acsphyschemau.2c00067
ACS Phys. Chem Au 2023, 3, 290−298